Modified effective-field approach to low-dimensional spin-1/2 systems

G. Kamieniarz,[1,*] R. Dekeyser,[2,†] G. Musiał,[1] L. Dębski,[1] and M. Bieliński[1]
[1]*Computational Physics Division, Institute of Physics, A. Mickiewicz University, ulica Umultowska 85, 61-614 Poznań, Poland*
[2]*Instituut voor Theoretische Fysica, Katholieke Universiteit Leuven, Celestijnenlaan 200D, B-3001 Leuven, Belgium*
(Received 7 January 1997)

Two different generalization schemes for the molecular field approximation are described. Both contain the possibility to incorporate generalized effective fields that induce correlations between the degrees of freedom at the boundary of a chosen cluster. Applications are presented for low-dimensional spin-1/2 systems. For the Ising models the critical couplings and critical exponents as well as the spontaneous magnetization curve are determined. An application of the method to the quantum $S=\frac{1}{2}$ one-dimensional Heisenberg model is presented and reliable low-temperature estimates of the specific heat are evaluated. The data are combined with the quantum transfer matrix predictions for large system sizes and this leads to the following prediction for the low-temperature specific heat: $C=AT^{\alpha}$ with $\alpha=0.35\pm0.07$. [S1063-651X(97)08006-9]

PACS number(s): 64.60.−i, 75.10.Hk, 75.10.Jm, 75.40.Mg

I. INTRODUCTION

The molecular field approximation (MFA) remains an important tool in the study of complex problems in solid-state physics and statistical mechanics. Whenever exact description of the critical behavior is impossible, usually a qualitative understanding of the phase diagram can be achieved within MFA [1,2]. In higher dimensions, where most of the sophisticated methods fail, MFA, in general, works better than in lower dimensions, and its predictions for the critical exponents become exact above the upper critical dimension. Due to its wide applicability, the mean field approach deserves further study. Especially in low dimensions many correction schemes have been undertaken to improve the accuracy of the MFA results.

In the present paper we summarize our ideas, previously presented in some preliminary reports [3,4], and we supplement them with some applications to both the classical Ising and the quantum Heisenberg model. We show how the notion of correlations can be embedded in the MFA approach and how the idea of the effective field with correlations can be merged with the exact finite-size calculations for quantum systems. Despite the relatively small system sizes available in the direct diagonalization technique, good estimates of the calculated quantities are obtained, when compared to the exact ones for the one-dimensional (1D) XY model [4,5] or to those well established in the literature [6–8], or even to those calculated here in the framework of the quantum transfer matrix. This demonstrates the advantages of the method for the investigation of the thermodynamic properties of low-dimensional spin systems and prompts us to calculate the low-temperature critical exponent for the specific heat of the 1D isotropic Heisenberg model. The conformal field theory has failed to give a conclusive answer in this case so far [9]. Some approximate theories, including the Bethe ansatz integral equation method, have yielded the spin wave value $\alpha=1/2$ [10–12] whereas the numerical techniques have predicted a lower value [13]. Our estimate $\alpha=0.35$ is consistent with that inferred from the Monte Carlo simulations [13].

II. FORMULATION OF THE METHOD

Let us consider first a classical spin system with short-range interactions. The lattice then can be divided into a finite cluster Ω, its boundary $\partial\Omega$, and the complement of $\Omega\cup\partial\Omega$ denoted by $\overline{\Omega}$. The Hamiltonian of the system can be written in the form

$$-\beta\mathcal{H}=H_0(\Omega,\partial\Omega)+H_1(\partial\Omega,\overline{\Omega}), \tag{1}$$

where $\beta=1/k_BT$ and k_B is the Boltzmann constant. This implies for the thermal expectation value of an operator A

$$\langle A\rangle=\sum_{\{\tau,\sigma,\bar{\sigma}\}} A(\sigma,\tau)e^{H_0(\sigma,\tau)+H_1(\tau,\bar{\sigma})}\Big/ \sum_{\{\tau,\sigma,\bar{\sigma}\}} e^{H_0(\sigma,\tau)+H_1(\tau,\bar{\sigma})}, \tag{2}$$

where the spin degrees of freedom are denoted as $\sigma\in\Omega$, $\tau\in\partial\Omega$, and $\bar{\sigma}\in\overline{\Omega}$. Hereafter we assume that $A=A(\sigma,\tau)$ and we aim at finding an efficient way for estimating the average (2). We follow two approaches.

In the first approach (the P scheme) the boundary $\partial\Omega$ is fixed in a particular state or is described by a probability distribution $P(\tau)$ so that the expectation value $\langle A\rangle$ is a weighted average

$$\langle A\rangle=\sum_{\{\tau\}} P(\tau)\left(\sum_{\{\sigma\}} Ae^{H_0}\Big/\sum_{\{\sigma\}} e^{H_0}\right). \tag{3}$$

The exact expression for $P(\tau)$ is given by

$$P(\tau)=\sum_{\{\sigma\}} e^{H_0(\sigma,\tau)}\sum_{\{\bar{\sigma}\}} e^{H_1(\sigma,\tau)}\Big/\sum_{\{\tau,\sigma,\bar{\sigma}\}} e^{H_0+H_1} \tag{4}$$

so that the probability distribution function $P(\tau)$ exists and can be written as

*Electronic address: gjk@pearl.amu.edu.pl
†Electronic address: raf.dekeyser@fys.kuleuven.ac.be

$$P(\tau)=2^{-N}\Bigg(1+\sum_i \langle\tau_i\rangle\tau_i+\sum_{\langle i,j\rangle}\langle\tau_i\tau_j\rangle\tau_i\tau_j + \sum_{\langle i,j,k\rangle}\langle\tau_i\tau_j\tau_k\rangle\tau_i\tau_j\tau_k+\cdots\Bigg), \quad (5)$$

where N is the number of all the τ spins and the prefactor ensures the normalization. The standard MFA consists in fixing the boundary spins and its distribution is given by the expression

$$P_0(\tau)=\prod_i \delta(\tau_i-m), \quad (6)$$

where m is a parameter calculated self-consistently from $m=\langle\sigma\rangle$. An improved choice [14,15] for the Ising model is

$$P_1(\tau)=2^{-N}\prod_i [(1+m)\delta(\tau_i-1)+(1-m)\delta(\tau_i+1)]$$

$$=2^{-N}\prod_i (1+m\tau_i), \quad (7)$$

where the variables τ_i are subject to the independent binary distributions. The probability distribution $P_1(\tau)$ can be easily obtained from the expression (5) by a simple decoupling of the correlations. Another decoupling $P_2(\tau)$ of the probability distribution function consists in

$$P_2(\tau)=2^{-N}\prod_i (1+a_i\tau_i)\prod_{i\neq j}(1+b_{ij}\tau_i\tau_j)\cdots, \quad (8)$$

where the coefficients b_{ij} take into account the correlations between the spins τ of the border. The symmetry of the cluster will be reflected in symmetry properties of these coefficients.

A second approach (the Q scheme) is formulated in the spirit of the mean-field theory. It is based on the idea that one may correct for the neglect of $\overline{\Omega}$ by introducing extra molecular fields acting on the boundary $\partial\Omega$ of the system and the thermal average

$$\langle A\rangle=\sum_{\{\tau,\sigma\}} Ae^{H_0(\sigma,\tau)+H'(\tau)}\Big/\sum_{\{\tau,\sigma\}} e^{H_0(\sigma,\tau)+H'(\tau)} \quad (9)$$

is determined by the effective field Hamiltonian $H'(\tau)$ defined as

$$e^{H'(\tau)}\equiv Q(\tau)=\sum_{\{\sigma\}} e^{H_1(\tau,\overline{\sigma})}. \quad (10)$$

This scheme would be exact if one could calculate the sum in Eq. (10). The standard cluster MFA [16] includes only the symmetry breaking fields in the effective Hamiltonian $H'(\tau)$ so that

$$Q_0(\tau)=\prod_i (1+a'\tau_i)\propto\exp\Big(a\sum_i \tau_i\Big). \quad (11)$$

The presence of an effective field a is due to the spontaneous symmetry breaking of the order parameter. The assumption of standard MFA is indeed that a is proportional to the order parameter $\langle\sigma\rangle$; therefore, we will call a the effective order parameter. An extension of the mean-field theory similar to our Q approach has been developed by Suzuki and applied in the context of the coherent anomaly method [17].

The function $Q(\tau)$ can also be expanded in a form such as Eq. (8), with coefficients that in general will be different from those appearing in the expansion of P. This implies that the effective Hamiltonian

$$H'(\tau)=\sum_i a_i\tau_i+\sum_{i,j} b_{ij}\tau_i\tau_j+\cdots, \quad (12)$$

apart from the standard linear term in τ, may also contain higher-order terms in τ, i.e., some correlations between the border spins.

To improve the simplest approximation, two scenarios can be followed both within the P approach of Eq. (4) or within the Q approach of Eq. (10), which are based on the concept of the self-consistent parameters and the series expansion technique. Self-consistent conditions can be imposed on the magnetization and the spin-spin correlation functions in order to determine the coefficients in P or Q. Correlations inside Ω may, e.g., be imposed to be equal to equivalent correlations inside $\partial\Omega$. Besides nearest-neighbor, also next-nearest neighbor or higher-order correlations may be considered. One should remark that, although the number of coefficients a_i, b_{ij}, ... in the exact expressions is finite, it is in general not possible to write down a closed set of self-consistency equations for them; the number of available equations is always smaller than the number of parameters. However, even in the lowest linear approximation in Eq. (12), our self-consistency condition $\langle\sigma\rangle=\langle\tau\rangle$ leads to some improvement with respect to MFA.

In the second scenario, standard series expansion techniques in expressions (4) or (10) can be applied and approximate expressions can also be found in the P and Q schemes for the correlations induced through H_1.

Both the P and Q approaches in the lowest order (equations (7) and (11), respectively) can be combined with the mean-field renormalization-group method (MFRG) [18], to obtain nonclassical critical exponents. The renormalization mapping $K'=K'(K,h)$, $h'=h'(K,h)$ is found from the scaling behavior of the cluster magnetizations in the P or Q approach. If $m_j(K,a,h)$ represents the magnetization of the jth system ($j=1,2$) for a given coupling K, an effective order parameter a and magnetic field h, and we define the rescaling factor l through $l^d=N/N'$ for two clusters with N and N' sites ($N>N'$), then within MFRG [18]

$$m_1(K',a',h')=l^{d-y_h}m_2(K,a,h),$$

where y_H is a critical exponent, and the effective order parameters fulfill $a'=l^{d-y_h}a$. Implementing MFRG, an attempt to include correlations in a self-consistent way may lead to some inconsistencies.

III. APPLICATIONS TO THE ISING MODEL

The efficiency of the method is demonstrated for the Ising models

TABLE I. The critical coupling K_c of the classical 2D Ising model found for different size L of the cluster. The second and third columns display the standard MFA and MFRG results. The fourth column contains the results obtained within the self-consistent P scheme, whereas the fifth and sixth columns contain those found from the P approach combined with the MFRG method on two and on three clusters, respectively. The seventh column shows the results evaluated within the self-consistent Q scheme, while the eighth and ninth columns illustrate the predictions obtained within the Q scheme by using series expansions and the Padé approximant technique for the correlation functions.

L	MFA	MFRG	P	P^{RG}	P_2^{RG}	Q	Q^P	$Q^{P\text{-RG}}$
1	0.250		0.324			0.346	0.408	
2	0.286	0.361	0.382	0.371		0.412	0.415	0.428
3	0.308	0.381	0.395	0.385	0.404	0.417		
4	0.323	0.393		0.395	0.418	0.420		
5	0.335	0.401						
	Exact				0.4407			

$$H=-K\sum_{\langle i,\delta\rangle}\sigma_i\sigma_{i+\delta}, \tag{13}$$

with nearest-neighbor interactions. Here $\langle i,\delta\rangle$ denotes that the summation runs over the nearest-neighboring pairs of spins.

At first, we consider clusters with L^d sites on the hypercubic lattices in $d=2$ and $d=3$ and we apply the P scheme. The critical couplings $K_c=J/k_BT_c$ are given in Tables I and II for $d=2$ and $d=3$, respectively. The cluster MFA and MFRG results are displayed in the second and third columns, respectively. In the fourth and fifth columns of Tables I and II our K_c predictions are given for the P approach with up to two correlations in Eq. (8) and for our implementation of MFRG in the framework of the P scheme on two L and $L-1$ clusters (denoted by P^{RG}). Moreover, the P^{RG} estimates are further improved in $d=2$, implementing a three cluster MFRG [19] (with L, $L-1$, and $L-2$ clusters), as demonstrated in the sixth column of Table I (denoted by P_2^{RG}).

TABLE II. The critical coupling K_c and the critical exponents in the framework of the P scheme for the classical 3D Ising model with different size L of the cluster. The second and third columns display the standard MFA and MFRG results. The fourth column shows the result calculated self-consistently without correlations. The fifth column shows an implementation of the MFRG method in the P scheme. The corresponding critical exponents y_T and y_H are presented in the seventh and ninth columns and preceded, for comparison, by the original MFRG ones.

L	MFA	MFRG	P	P^{RG}	MFRG	P^{RG}	MFRG	P^{RG}
					y_T		y_H	
1	0.167		0.197					
2	0.182	0.207		0.209	0.82	0.902	2.00	1.997
3	0.191	0.212			0.95		2.08	
	Exact	0.22165			1.59		2.484	

TABLE III. The critical exponents y_T and y_H of the 2D Ising model for different linear size L of the cluster. MFRG denotes the results obtained by using the MFRG method. P^{RG} and P_2^{RG} denote the results of the P scheme combined with the MFRG method on two and on three clusters, respectively. The columns denoted by $Q^{P\text{-RG}}$ contain the estimates of the Q scheme and Padé approximant analysis in conjunction with MFRG.

L	MFRG	P^{RG}	P_2^{RG}	$Q^{P\text{-RG}}$	MFRG	P^{RG}	P_2^{RG}	$Q^{P\text{-RG}}$
		y_T				y_H		
2	0.69	0.822		0.801	1.50	1.490		1.715
3	0.78	0.930	0.942		1.57	1.585	1.609	
4	0.82	0.979	0.996		1.60	1.636	1.676	
5	0.84				1.62			
	Exact	1.000			1.875			

The critical exponents y_T and y_H for the thermal and ordering fields follow from the linearized recursion relations and are given in the corresponding columns of Table III for $d=2$ and Table II for $d=3$.

For the Q and P schemes, we have performed self-consistent calculations in 2D including the pair correlations up to the third neighbors. In Table IV the variation of critical coupling K_c is shown for different system sizes L and different number of correlations within the Q approach. The total number of correlations n is specified in the first column. When $n=0$, only symmetry breaking fields are present. In the last row, three successive correlations are taken into account and the self-consistency conditions require cluster with linear size $L\geqslant 3$. The best results found self-consistently for different cluster sizes were already used in Table I. Those found from the P approach are given in the fourth column, whereas those from the Q approach are in the seventh column.

Next we report some self-consistent results for the triangular lattice, which is especially suited for our methods, and we approximate both P and Q by an expression such as Eq. (8). We choose an Ω cluster consisting of a single site with spin variable σ whereas its six nearest neighbors with spin variables τ form the border $\partial\Omega$. The results for K_c in both approaches are given as P^{sc} and Q^{sc} in Table V. In the first approximation, referred to as order 1, a is determined by imposing $\langle\sigma\rangle=\langle\tau\rangle$ and $b=0$; in the second approximation b is determined through $\langle\sigma\tau\rangle=\langle\tau_1\tau_2\rangle$. These estimates of K_c should be compared with the simple mean-field result $K_c\approx 0.1667$ and the exact $K_c\approx 0.2746$. In the second ap-

TABLE IV. The critical couplings K_c in the framework of the Q and P schemes for the 2D Ising model with different linear size L of the cluster. The number of succeeding correlations n included in self-consistent calculations is defined in the first column.

	Q scheme				P scheme		
n	$L=1$	$L=2$	$L=3$	$L=4$	$L=1$	$L=2$	$L=3$
0	0.346	0.353	0.368	0.378	0.324	0.342	0.355
1		0.376	0.392	0.400		0.361	0.370
2		0.412	0.414	0.416		0.382	0.395
3			0.417	0.420			

TABLE V. Estimates for the critical coupling K_c for the triangular Ising model. The second and third columns illustrate the self-consistent P and Q predictions with no correlations (the first order) and the nearest-neighbor correlations (the second order), respectively. In the last two columns the estimates calculated by using series expansions (Q^{se}) and the Padé approximant technique (Q^P) are given.

Order	P^{sc}	Q^{sc}	Q^{se}	Q^P
1	0.197	0.2025	0.2270	0.2270
2	0.226	0.2522	0.2373	0.2415
3			0.2441	0.2542
4			0.2498	0.2562
Exact		0.2746		

proximation, it turns out that the pair correlation $\langle\sigma\tau\rangle$ is finite and attains at criticality the value 0.492, which is of the correct order of magnitude with respect to the exact value 0.667.

We report also the results found from a series expansion of Q on the same triangular lattice. In the definition (10) of Q we write

$$e^{K\overline{\sigma_i\sigma_j}}\propto(1+x\overline{\sigma_i\sigma_j}),$$

with $x=\tanh K$, and we expand the correlation factors in ascending powers of x. It can be noticed that Q contains a factor $(1+b\tau_i\tau_j)$ for each pair of nearest neighbors in $\partial\Omega$ and an extra factor $(1+c\tau_i\tau_j)$ for each next-nearest-neighbor pair, with

$$b=x(1+x+2x^2+4x^3+\cdots)$$

$$c=x^4+\cdots. \tag{14}$$

The series expansion results for K_c are given in the fourth column of Table V, referred to as Q^{se}. Here various approximations are obtained for Q, defined by the order in x of the parameters b and c. In Table V we present the variation of K_c according to the number of terms kept in Eq. (14). Furthermore, each approximation may be improved by replacing b by a corresponding Padé approximant in x. These results, referred to as Q^P, are displayed in the fifth column of Table V.

Similar series expansion calculations are carried out for the square lattice. We have evaluated the magnetization per site m_1 and m_2 for $L=1$ and $L=2$ clusters, using pair correlation functions up to the sixth order in x,

$$\langle\sigma_a\sigma_b\rangle\approx x+x^3+2x^5+\cdots,$$

$$\langle\sigma_b\sigma_c\rangle\approx x^2(1+2x^2+4x^4+\cdots), \tag{15}$$

where a and b denote the nearest-neighbor sites whereas b and c represent the next-nearest-neighbor sites. Using Padé approximants we have obtained the critical couplings given in the column labeled Q^P in Table I. We remark that there is a fifth-order next-nearest-neighbor correlation in the larger system.

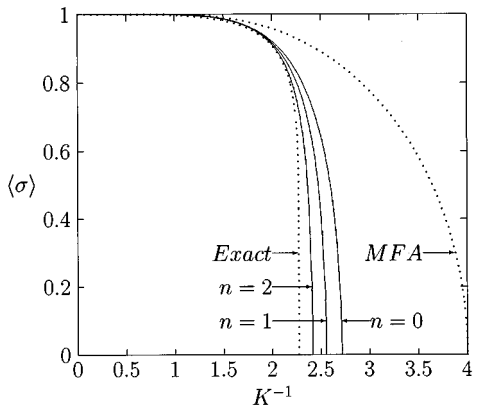

FIG. 1. The magnetization as a function of $K^{-1}=k_BT/J$ for 2D Ising model.

The corresponding series expansions for Q may also be combined with the MFRG method on two clusters consisting of $N'=1$ and $N=4$ sites. This simple procedure leads to rather accurate estimates of K_c (the column denoted by $Q^{P\,-\mathrm{RG}}$ in Table I) and the critical exponents y_T and y_H (Table III). An intriguing question is whether the values obtained for y_T really converge to 1, or overshoot this exact value. Unfortunately, calculations for $L\geqslant 5$ are at present not feasible; calculations on too large clusters are furthermore not in the spirit of the present approach.

Our approach is also a suitable tool for the calculation of the temperature-dependent thermodynamic properties of the Ising model. The magnetization profiles are presented in Fig. 1. The lower dotted curve is drawn according to the exact result of Yang [20] while the upper one illustrates the standard MFA predictions. The solid curves lying in between have been calculated here within the Q scheme for a $L=3$ cluster. The label n represents the number of succeeding pair correlations included in our approach. The upper curve demonstrates the behavior of magnetization found from the self-consistent calculations with no correlations between border spins. The middle one, labeled $n=1$, represents our Q predictions if only nearest-neighbor correlations are included. The remaining $n=2$ curve shows the magnetization profile if both the nearest- and the next-nearest-neighbor correlations are included in Q. For the sake of clarity, we have only plotted in Fig. 1 our magnetization curves for $L=3$. The improvement of the magnetization behavior is also very systematic with each subsequent number of correlations taken into account for smaller clusters.

The Q approach of Eq. (10) proves to be the most efficient. This is most pronounced in one-dimensional problems, where the Q method yields exact results for classical 1D Ising systems in a magnetic field. This success is due to the fact that H' contains only those correlations that come from interactions through $\overline{\Omega}$ and not those from interactions through Ω. The correlation between the leftmost and rightmost site of a finite segment of a line, however, is completely due to interactions through this segment. If τ_1 and τ_2 are the two boundary spins of the segment, this means that $Q(\tau_1,\tau_2)$ does not contain any correlation and factorizes as $Q=q(\tau_1)q(\tau_2)$. The function $q(\tau)$ can then be determined

by a recursive argument and this makes the Bethe scheme exact in one dimension, where H' consists only of a simple molecular field $h(\tau_1+\tau_2)$.

IV. APPLICATION TO THE QUANTUM HEISENBERG MODEL

For quantum mechanical models, the factor $\exp(H_1)$ in general cannot be extracted from the Boltzmann factor. Instead, we should define

$$e^{H_0+H'}=\sum_{\sigma} e^{H_0(\sigma,\tau)+H_1(\tau,\overline{\sigma})}, \tag{16}$$

where H' may also depend on the variables σ from the interior of the cluster Ω.

Approximate expressions for H' may be derived from Eq. (16) using, e.g., the Baker-Campbell-Hausdorff formula or Feynman's identity. The previous mean-field-like scenario is also possible here, if the strongest contributions to H' appear at or around the boundary $\partial\Omega$. By symmetry arguments, the form of the most important terms in H' can then be imposed and its parameters can be determined through self-consistency conditions. The first successful applications of this scenario have been undertaken for the XY model [4].

In this work we follow the mean-field scenario and we use our method in conjunction with the finite-chain diagonalization technique for the Heisenberg model. The exact diagonalization technique has been widely used for the low-dimensional spin systems [6,8,21]. At higher temperatures the extrapolation technique yields then very consistent predictions in the macroscopic limit. The convergence of the extrapolations deteriorates with decreasing temperature. Our aim is to improve the convergence of the low-temperature specific heat predictions.

As to the 1D isotropic Heisenberg model, there is no broken symmetry in this model and we have no external field in H'. We expect the main contribution to H' in the form of additional Heisenberg interactions between the spins at the edges of the finite segment. Thus the effective Hamiltonian can be chosen in the form

$$H_0+H'\approx\frac{1}{2}K\sum_{i=1}^{N-1}\vec{\sigma}_i\cdot\vec{\sigma}_{i+1}+\frac{1}{2}\sum_{i=1}^{L}K_i(\vec{\sigma}_i\cdot\vec{\sigma}_{i+1}+\vec{\sigma}_{N-i}\cdot\vec{\sigma}_{N-i+1}), \tag{17}$$

where K denotes the bare couplings and the K_i denote the additional nearest-neighbor couplings for the external sectors of the chain of the length N. L is the number of such additional terms taken into account (evidently, we must choose $L\leqslant N/2$). $\vec{\sigma}$ represents here the vector of the Pauli spin matrices. The couplings K_i are subject to self-consistency conditions for the corresponding correlation functions: we must impose that the nearest-neighbor correlations in the external sectors are equal to the average correlation function in the internal segment.

Using our method we have calculated the zero-field specific heat C of the model under consideration in a wide temperature region, performing direct diagonalization with free boundary conditions. The results illustrated by dots in Fig. 2 yield the smooth curve and are consistent with those found previously [6–8]. For every considered point in the region $k_BT/J\leqslant 2.0$, computations were carried out by the standard finite-segment calculations, i.e., with no additional Heisenberg interaction included at the ends of a chain ($2\leqslant N\leqslant 15$) as well as with up to 2 extra effective couplings K_i included. For $k_BT/J\geqslant 2.0$ only the standard finite segment calculations have been performed and the results coincide with those found from the high-temperature expansions [7]. We have found the extrapolated data plotted in Fig. 2 for three different approximations (17)—the one with no extra interactions in the external sectors and those with $L=1$ and $L=2$ additional interactions. As an example, Fig. 3 shows the variation of the finite-size specific heat estimates C (per site, in units of k_B) with respect to $1/N$ for $k_BT/J=0.1$. The standard finite chain results are illustrated by the squares in Fig. 3. The results obtained with one and two self-consistent parameters are given by triangles and asterisks, respectively.

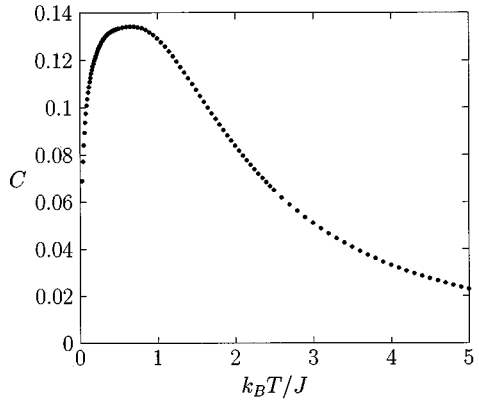

FIG. 2. The zero-field specific heat per site for the isotropic 1D Heisenberg model.

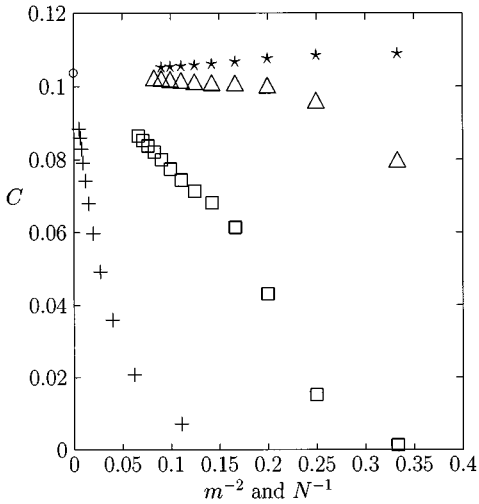

FIG. 3. Variation of the zero-field specific heat per site at $k_BT/J=0.1$ against $1/N$ for the finite-chain diagonalization data ($3\leqslant N\leqslant 15$; the symbols □, △, and ⋆ represent the standard, one- and two-parameter approximation, respectively) and against $1/m^2$ for the transfer-matrix data (+ symbols, $3\leqslant m\leqslant 13$). All data converge towards the point denoted by a circle.

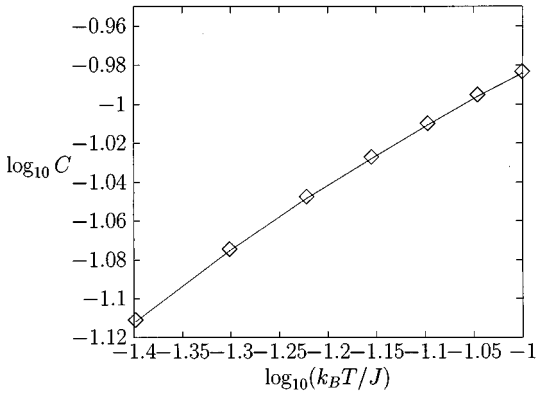

FIG. 4. The logarithm of the zero-field specific heat per site for the 1D Heisenberg model vs the logarithm of k_BT/J.

One can see a good convergence of the data towards the extrapolated value denoted by a circle in Fig. 3. The effective interactions K_i at the ends of the chain improve the convergence and yield consistent estimates of the extrapolated values down to $k_BT/J=0.04$ with an accuracy higher than before [6].

In order to verify our results in the low-temperature region ($k_BT/J\leqslant 1.0$), we have also performed extensive quantum transfer-matrix (QTM) [22] calculations based on the real-space decomposition. The details of the technique can be found elsewhere [22,23]. We have considered chains with length up to $N=360$ and we have reached the size m in the Trotter direction ($m\leqslant 13$) far beyond what we are aware of in the literature. An example of our QTM data is included in Fig. 3 and plotted by crosses against $1/m^2$. We have found our QTM extrapolated values in $1/m^2$ consistent with our effective-field results based on the approximation (17). Actually, despite the large system sizes reached in our QTM calculations, the data follow a rather steep curve and do not diminish the uncertainty (below 1% in the lowest temperatures) found from the finite-chain extrapolations.

We would like to exploit the high accuracy of our specific-heat results and to extract the corresponding critical exponent α in the zero-temperature limit. The low-temperature behavior of the specific heat in the log-log scale is illustrated in Fig. 4 for $0\leqslant k_BT/J\leqslant 0.1$. Our numerical data are represented by diamonds and are connected by a straight line. Due to the observed nonlinearity, corrections to scaling in the form

$$C=AT^{\alpha}(1+B\ln^{\beta}T) \tag{18}$$

have to be taken into account. We have tried first the power-law correction term but we concluded that our data allow only logarithmic corrections. We have fitted the scaling form (18) to our numerical data for a given number n of the data points starting from the reference temperature k_BT_0/J. As the distance Δ between successive temperatures amounts to 0.01, we have fixed k_BT_0/J and we have performed the fitting procedure in the temperature region $n\Delta$. The results of our analysis are given in Table VI, where the first column contains the reference temperature and the second column specifies the width of the temperature region. The unknown critical exponents and amplitudes are collected in the remaining part of Table VI. The data for the leading exponent α and the corresponding amplitude A are consistent and enable a conclusion $\alpha=0.36\pm 0.06$ and $A=0.20\pm 0.03$.

TABLE VI. Scaling analysis of the low-temperature numerical specific heat data. The fitting is carried out in the temperature region starting from k_BT_0/J and the width $0.01n$. The leading critical exponent is denoted by α, the corresponding amplitude by A, the subleading exponent by β, and the corresponding amplitude by B.

k_BT_0/J	n	α	A	β	B
0.04	7	0.357	0.185	0.480	0.190
0.04	12	0.320	0.180	0.501	0.130
0.04	15	0.304	0.175	0.494	0.120
0.05	7	0.367	0.184	0.673	0.182
0.05	12	0.382	0.210	0.017	0.188
0.06	7	0.337	0.177	0.541	0.174

Another attempt to find the exponent α is related to some thermodynamic considerations for the specific heat and the total entropy gain. As to the specific heat,

$$\int_0^{\infty} C(T)dT=U(\infty)-U(0)=0.5, \tag{19}$$

where $U(T)$ means the internal energy in units of the interaction parameter J. This integral can be calculated numerically under a smooth curve spanned over our numerical data $C(T)$, starting from a certain temperature T_0. In order to estimate the corresponding contribution for $T\leqslant T_0$, the $C(T)$ dependence is approximated by the leading term in Eq. (18). Referring to the condition (19) and imposing continuity at $T=T_0$, the unknown amplitude A and the critical exponent α can be evaluated. The calculations were performed for different values of k_BT_0/J in order to estimate the uncertainty of our solutions. Taking into regard the scatter of the results presented in the second and third columns of Table VII, we get $\alpha=0.33\pm 0.02$ and $A=0.23\pm 0.02$.

We can also estimate numerically the total entropy gain, which amounts to ln2. Assuming the power-law behavior of the specific heat in the low-temperature limit and the relation $dS=C(T)dT/T$, the values of the parameters α and A can be found in a similar way as before. In this case the low-temperature contribution to the integral is significantly en-

TABLE VII. Estimates of the specific-heat critical exponent α and the amplitude A obtained from a numerical analysis of the thermodynamic identities. For different intermediate temperatures k_BT_0/J the second and third columns present the results when the identity for the specific heat C is exploited, whereas the fourth and fifth columns present those for the entropy S.

k_BT_0/J	α	A	α	A
	C		S	
0.04	0.332	0.225	0.412	0.291
0.05	0.341	0.234	0.409	0.286
0.06	0.343	0.235	0.404	0.279
0.07	0.334	0.228	0.398	0.270

hanced. After analysis of these results (Table VII, the fourth and fifth columns) we have obtained $\alpha = 0.41 \pm 0.02$ and $A = 0.29 \pm 0.02$.

Taking into account our analysis we end up with the conclusion

$$\alpha = 0.35 \pm 0.07 \quad \text{and} \quad A = 0.23 \pm 0.05. \tag{20}$$

V. CONCLUSIONS

We have presented a effective-field approach applicable to classical and quantum systems with short-range interactions. In the classical limit the thermal average is either expressed as the weighted mean value for fixed configurations of the border spin variables (the P approach) or it is given by an effective Hamiltonian (the Q approach). The effective hamiltonian is acting on the border spin variables τ and may contain higher-order terms in τ (i.e., correlations) with corresponding coefficients. We have proposed a systematic way to calculate these coefficients either by imposing some self-consistent conditions on the correlation functions or by exploiting the series expansion technique. We have accomplished a much faster improvement with respect to the MFA predictions by increasing the order of approximation than by increasing the size of the cluster. For quantum systems we have considered a variant of the Q approach and we have defined an effective Hamiltonian with extra nearest-neighbor interactions at the end of the chain.

As an illustration we have applied our approach to the classical Ising model and to the 1D Heisenberg model. We have seen for the Ising model a systematic improvement of our predictions for the critical coupling K_c and the critical exponents (implementing MFRG) both for the P and the Q approach. In the quantum case we have evaluated the specific heat and we have extracted the corresponding critical exponent. We have confirmed our low-temperature estimates of the specific heat by large-scale QTM calculations so that we have found from our numerical computations strong evidence that $\alpha < 1/2$. We have also tried to reanalyze the known high-temperature series [7] but we have not reached firm conclusions.

ACKNOWLEDGMENTS

The authors thank Professor H. Blöte and Professor J. Rogiers for some discussions and gratefully acknowledge the access to SGI Power Challenge XL, Cray YMP-EL, and Cray J916 in the Supercomputing and Networking Center in Poznań. Partial financial support of the Committee for Scientific Research within the Grant 2 P302 116 06 and a grant from the Flemish Foundation for Scientific Research (FWO) is also acknowledged.

[1] C. Domb, Adv. Phys. **9**, 149 (1960); J.S. Smart, *Effective Field Theories of Magnetism* (Saunders, Philadelphia, 1966).
[2] D.M. Burley, in *Phase Transitions and Critical Phenomena*, edited by C. Domb and M.S. Green (Academic Press, London, 1972).
[3] R. Dekeyser, and G. Kamieniarz, J. Magn. Magn. Mater. **104-107**, 273 (1992)
[4] G. Kamieniarz, R. Dekeyser, and G. Musiał, Acta Phys. Pol. **85**, 413 (1994)
[5] S. Katsura, Phys. Rev. **127**, 1508 (1962)
[6] H.W.J. Blöte, Physica B **79**, 427 (1975)
[7] T. de Neef, Phys. Rev. B **13**, 4141 (1976)
[8] J.C. Bonner and M.E. Fisher, Phys. Rev. **135**, A640 (1964)
[9] A. Klümper and P.A. Pearce, Physica A **194**, 397 (1993)
[10] M. Takahashi, Phys. Rev. Lett. **58**, 168 (1987)
[11] P. Schlottmann, Phys. Rev. B **33**, 4880 (1986)
[12] M. Yamada and M. Takahashi, J. Phys. Proc. Jpn. **55**, 2024 (1986)
[13] J.W. Lyklema, Phys. Rev. B **27**, 3108 (1983)
[14] H. Mamada and F. Takano, J. Phys. Soc. Jpn. **25**, 675 (1968)
[15] A. Benyoussel and N. Boccara, J. Phys. Oceanogr. **44**, 1143 (1983)
[16] H.A. Bethe, Proc. R. Soc. London, Ser. A **150**, 552 (1935)
[17] M. Suzuki, X. Hu, M. Katori, A. Lipowski, N. Hatano, K. Minami, and Y. Nonomura, *Coherent Anomaly Method. Mean Field, Fluctuations and Systematics* (World Scientific, Singapore, 1995), p. 22.
[18] J.O. Indekeu, A. Maritan, and A.L. Stella J. Phys. A **15**, L291 (1982)
[19] J.O. Indekeu, A. Maritan, and A.L. Stella, Phys. Rev. B **35**, 305 (1987)
[20] C.N. Yang, Phys. Rev. **85**, 808 (1952)
[21] L.S. Campana, A. Caramico D'Auria, U. Esposito, G. Kamieniarz and R. Dekeyser, Phys. Rev. B **42**, 10 765 (1990)
[22] T. Delica and H. Leschke, Physica A **168**, 736 (1990)
[23] L.S. Campana, A. Caramico D'Auria, F. Esposito, U. Esposito, and G. Kamieniarz, Phys. Rev. B **53**, 2594 (1996).